AJNR

# Diffusion-weighted MR imaging of the brain: value of differentiating between extraaxial cysts and epidermoid tumors.

J S Tsuruda, W M Chew, M E Moseley and D Norman

*AJNR Am J Neuroradiol* 1990, 11 (5) 925-931
http://www.ajnr.org/content/11/5/925

# Diffusion-Weighted MR Imaging of the Brain: Value of Differentiating Between Extraaxial Cysts and Epidermoid Tumors

Jay S. Tsuruda[1]
Wil M. Chew
Michael E. Moseley
David Norman

**This study demonstrates the use of diffusion-weighted MR imaging in improving the specificity of the diagnosis of extraaxial brain tumors. Three surgically proved lesions (one arachnoid cyst and two epidermoid tumors) and two nonsurgically proved lesions (arachnoid and ependymal cysts) were evaluated with T1- and T2-weighted spin-echo studies followed by intravoxel incoherent motion (IVIM) MR imaging. The IVIM images of the lesions were displayed as an apparent diffusion coefficient (ADC) image obtained at 0.65 G/cm (maximum gradient b value = 100 sec/mm$^2$) and compared with external oil and water phantoms. The ADC of arachnoid cysts was similar to stationary water whereas the ADC of epidermoid tumors was similar to brain parenchyma, indicating the solid nature and the slower diffusion rate of the epidermoid tumors. Cisternal CSF demonstrated uniformly high ADC, primarily because of bulk flow, which enhanced image contrast. Improved delineation of postsurgical changes was also possible.**

**Our preliminary results show that diffusion-weighted MR imaging can be useful in distinguishing between arachnoid cysts and epidermoid tumors.**

***AJNR* 11:925–931, September/October 1990; *AJR* 155: November 1990**

The application of strong magnetic field gradients during proton MR imaging allows one to observe differences in molecular self-diffusion [1]. The basis for this diffusion is molecular translational (Brownian) motion, which leads to attenuation of signal intensity in each image voxel. Proton diffusion rates differ according to the tissue type; and specific techniques, such as intravoxel incoherent motion (IVIM) imaging, resulting in an apparent diffusion coefficient (ADC) image, have been developed to exploit these differences [1]. Early findings with diffusion-weighted imaging of normal patients [1–8] have yielded variable results in quantifying diffusion differences between CSF, gray matter, and white matter. Preliminary examples of intraparenchymal tumors and associated edema [1, 3, 5, 6], infarcts [1, 7], normal pressure hydrocephalus [7], and benign intracranial hypertension [1, 7, 8] have shown regions of either increased or restricted diffusion when compared with normal parenchyma.

Clinical application of this technique is significantly hindered by physiological pulsatile and uncontrolled patient motion. Artifacts generated by motion limit quantitative measurements and differentiation of critical anatomic structures; for example, gray/white matter interfaces [6]. This motion-generated artifact may be used to advantage in the case of in vivo macroscopic CSF motion, where the apparent diffusion value of CSF is increased when compared with stationary fluid [2]. This phenomenon may assist in accentuating image contrast between normal CSF and extraaxial tumors on a diffusion-weighted image. Additionally, further characterization of a mass lesion based on intrinsic diffusion values should be possible.

The purpose of this study was to demonstrate the utility of ADC imaging in improving conspicuity and specificity of extraaxial lesions in three surgically proved cases. We applied the knowledge gained from these three cases to assist in the

Received September 23, 1989; revision requested December 14, 1989; revision received February 5, 1990; accepted February 22, 1990.

Presented at the annual meeting of the Society of Magnetic Resonance in Medicine, Amsterdam, August 1989.

[1] All authors: Department of Radiology, Box 0628, 505 Parnassus Ave., University of California School of Medicine, San Francisco, CA 94143. Address reprint requests to J. S. Tsuruda.

0195-6108/90/1105–0925

therapeutic management of two nonsurgically proved cases. The limitations of this technique and some pitfalls in image interpretation are also described.

## Material and Methods

All studies were performed on a 1.5-T GE Signa system using a self-shielded RF gradient coil (1 G/cm maximum) and standard quadrature head coil. Prior to scanning, the patients were immobilized within the head coil with a vacuum-assisted device (size 20, Olympic Medical, Seattle, WA). In the majority of patients, an external phantom consisting of plastic tubing filled with mineral oil and water was simultaneously imaged. Care was taken to position the phantom such that it would be seen on any orthogonal slice through the brain. Acetone was also included as an external reference in one patient. All patients were initially studied with a multislice T1-weighted sagittal sequence, 600/20/2 (TR/TE/excitations), 5-mm-thick slices, 1-mm interslice gap, 22-cm field of view, and 192 × 256 matrix. This was followed by a multislice, multiecho T2-weighted sequence (2800/30,80/1), 5-mm thick, 2.5-mm interslice gap, 20-cm field of view, and 192 × 256 matrix. Gradient-moment nulling (Flow Compensation, General Electric) without cardiac gating was used on the long TR images. Additional T1-weighted sagittal and coronal images were obtained if additional anatomic detail was desired.

Multislice ADC images [1] were obtained in the axial plane using a cardiac-gated spin-echo sequence 900–1000 (effective TR)/100/2–4. The diffusion-gradient pulse duration was 30 msec with a gradient separation of 43 msec and a maximum gradient strength of 0.65 G/cm corresponding to a maximum gradient b value of approximately 100 sec/mm$^2$ [3]. The final ADC image reflects the ratio of signal intensities between two images obtained with either high b and low b gradient values. This method has been previously described in detail [1]. The diffusion gradient was applied along the frequency-encoding axis, which was oriented along the anterior-posterior direction on axial sections and along the superior-inferior direction on both the sagittal and coronal sections. Slice thickness was 5 mm with a field of view of 24 cm and a 128 × 256 matrix. Imaging time was approximately 8–13 min.

In three patients, surgical confirmation of the MR findings was obtained. In addition, the second patient also underwent axial and coronal CT cisternography immediately after a lumbar intrathecal injection of 5 ml of iohexol (Omnipaque 240, Winthrop). The fourth and fifth patients were also studied by contrast-enhanced MR immediately following IV injection of 0.1 mmol/kg gadopentetate dimeglumine (Magnevist, Berlex).

## Results

### *Patient 1*

A 40-year-old woman presented with a 1-year history of vertigo, nausea, right ear pain without hearing loss, and transient right upper extremity numbness with poor coordination. Short and long TR spin-echo images demonstrated a mass in the right cerebellopontine angle and lateral medullary cisterns with extrinsic compression of the brainstem and isointensity with CSF in all sequences (Figs. 1A–1C). On the

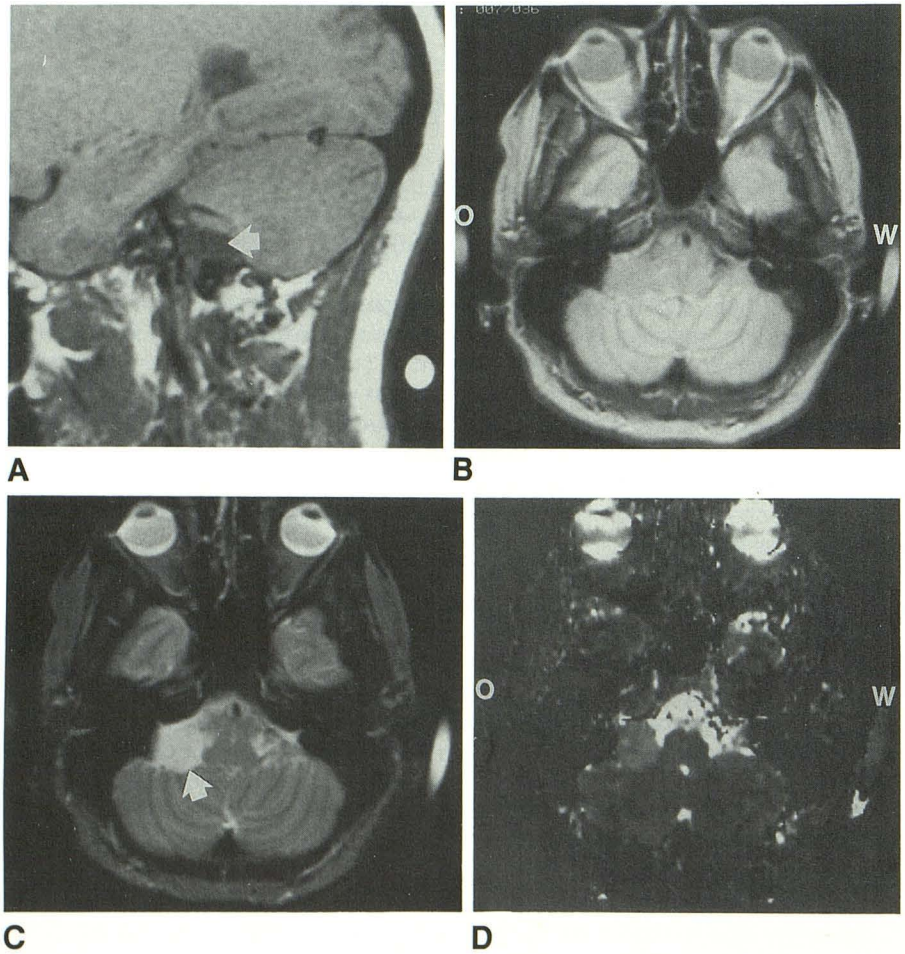


**Fig. 1.—Patient 1: Arachnoid cyst of the posterior fossa.**

***A*, Parasagittal T1-weighted image (600/20) shows widening of right cerebellopontine angle cistern (*arrow*). Note that a portion of the external oil phantom is seen posterior to upper neck.**

***B* and *C*, T2-weighted images (2800/30/80) confirm the presence of an extraaxial mass (*arrow* in *C*) of CSF signal intensity. Portions of the oil (O) and water (W) phantoms are shown.**

***D*, Apparent diffusion coefficient (ADC) image (gated/100) shows a distinct boundary between cisternal CSF and the mass, which is higher in signal intensity than adjacent cerebellum but similar in intensity to stationary water phantom (W). The oil phantom shows nearly complete loss of signal, compatible with its relatively slow diffusion constant. The increased signal within the eyes is due to orbital motion during image acquisition, causing an increase in the ADC. Slight heterogeneity of signal intensity is noted in lateral aspect of both cerebellar hemispheres due to phase artifact generated from orbital motion projecting posteriorly.**

ADC images, the mass was isointense with the stationary water phantom, and had slightly greater intensity compared with normal brain parenchyma. Cisternal CSF exhibited greater intensity than the stationary water phantom (Fig. 1D). The interface and contrast between the mass and the cistern was well defined. Because of the similarity in ADC signal intensity between the mass and stationary water, a diagnosis of a locculated fluid collection, compatible with an arachnoid cyst, was suggested and subsequently confirmed surgically.

*Patient 2*

A 55-year-old man who had had surgical resection of an intracranial epidermoid tumor at age 35 presented with complaints of progressive visual loss. A recurrence of the tumor was suspected clinically. Short and long TR spin-echo MR images (Figs. 2A–2F) showed an intraaxial anteromedial left frontal lesion and the suggestion of an extraaxial suprasellar lesion extending into the middle cranial fossa; both were isointense with CSF on all sequences.

CT cisternography (Figs. 2G–2J) demonstrated a CSF density mass in the suprasellar cistern, enlarged CSF spaces in the medial aspect of the left temporal lobe, and low density in the frontal lobe, the latter compatible with either encephalomalacia due to prior surgery or, less likely, epidermoid tumor. With CT cisternography, discrimination between enhancing cisternal CSF and tumor was possible; however, the low-density encephalomalacia could not be distinguished from the cisternal mass.

The ADC images (Figs. 2K–2M) showed uniformly increased signal intensity of the cisternal CSF, markedly decreased signal within the tumor (similar to normal brain parenchyma), and intermediate signal within the encephalomalacia. Orbital motion, resulting in phase artifact, degraded the phantom images, so quantitative comparison with tumor was not possible. However, qualitatively the ADC study indicated that the cisternal mass was solid in nature, indicating recurrence of epidermoid tumor and that separation between tumor and encephalomalacia was possible. These findings were confirmed surgically.

*Patient 3*

A 58-year-old woman was evaluated by MR for the diagnosis of left-sided tic douloureux. The short TR and long TR spin-echo MR images (Figs. 3A and 3B) demonstrated an asymmetric widening of the left cerebellopontine angle cistern with a mass of CSF-like intensity. Morphologically, this lesion most likely represented an epidermoid tumor; however, an arachnoid cyst could not be entirely excluded. The axial ADC image (Fig. 3C) revealed that the lesion was heterogeneous with signal intensity predominantly similar to brain parenchyma as opposed to either stationary water or cisternal CSF. The ADC image identified the solid nature of the mass and confirmed the presence of an epidermoid tumor, which was proved surgically.

*Patient 4*

A 5-year-old boy presented with a history of petit mal seizures, which were well controlled by medication. ECG indicated bihemispheric epileptogenic foci. Short and long TR images demonstrated a well circumscribed mass with intensity similar to CSF filling the right temporal horn and extending into the adjacent choroidal fissure. A preliminary diagnosis of an atypical arachnoid cyst was made. The ADC study (Fig. 4) confirmed the presence of stationary fluid intensity. The patient will be electively followed without surgical intervention.

*Patient 5*

A 26-year-old man presented with a several-month history of progressive dizziness associated with nausea and vomiting. The screening MR scan demonstrated moderate third and lateral ventriculomegaly requiring decompression by shunt tube placement and a mass in the posterior third ventricle, which was isointense with CSF. There was no enhancement on the postcontrast examination. The ADC image confirmed that this lesion behaved similarly to the stationary water phantom. The presumptive diagnosis was that of a third ventricular ependymal cyst rather than a solid neoplasm. Since ependymal cysts are a benign process, the patient will be electively followed without any further surgical intervention at this time.

## Discussion

IVIM MR imaging, first described by Le Bihan and coworkers [3], is a method of obtaining images sensitive to microscopic translational motions that occur in each MR imaging voxel. The effect of IVIM is to cause an apparent reduction of the spin-echo signal and therefore a reduction of signal intensity. In biological tissue, this reduction is thought to be due primarily to molecular self-diffusion and perfusion (capillary flow). IVIM may be quantified by the use of different gradient b values [9] for different sequences (keeping all other parameters identical). In this fashion, magnitude images with differing b values are obtained. From two resulting magnitude images, an ADC image is constructed. In this study, we found that the ADC image was preferred over the magnitude image, since image contrast is independent of spin density, T1, and T2 differences. On the ADC image, relative signal intensity is due to differences in tissue diffusion and perfusion (if present). By using this method, one can calculate reproducible diffusion coefficients, in units of $10^{-5}$ $cm^2$/sec, of stationary fluids such as acetone, oil, water, and cyclohexane and compare them favorably with published values [10].

The application of ADC imaging in vivo has been met with limited success because of artifacts [6]. This image degradation is caused by the presence of coherent or incoherent macroscopic motion from either gross patient motion and/or physiological brain motion due to cardiac or respiratory pulsations. This increased sensitivity to patient motion is accentuated by the long imaging times required to obtain a diffusion-weighted spin-echo image [4]. An attempt was made to reduce unwanted motion by immobilizing the patient with a vacuum device originally suggested by Thomsen and coworkers [7]. An occasional image artifact was still present in some of our clinical cases, resulting in degradation of parenchymal detail with associated nonuniformity of signal intensity (Figs.

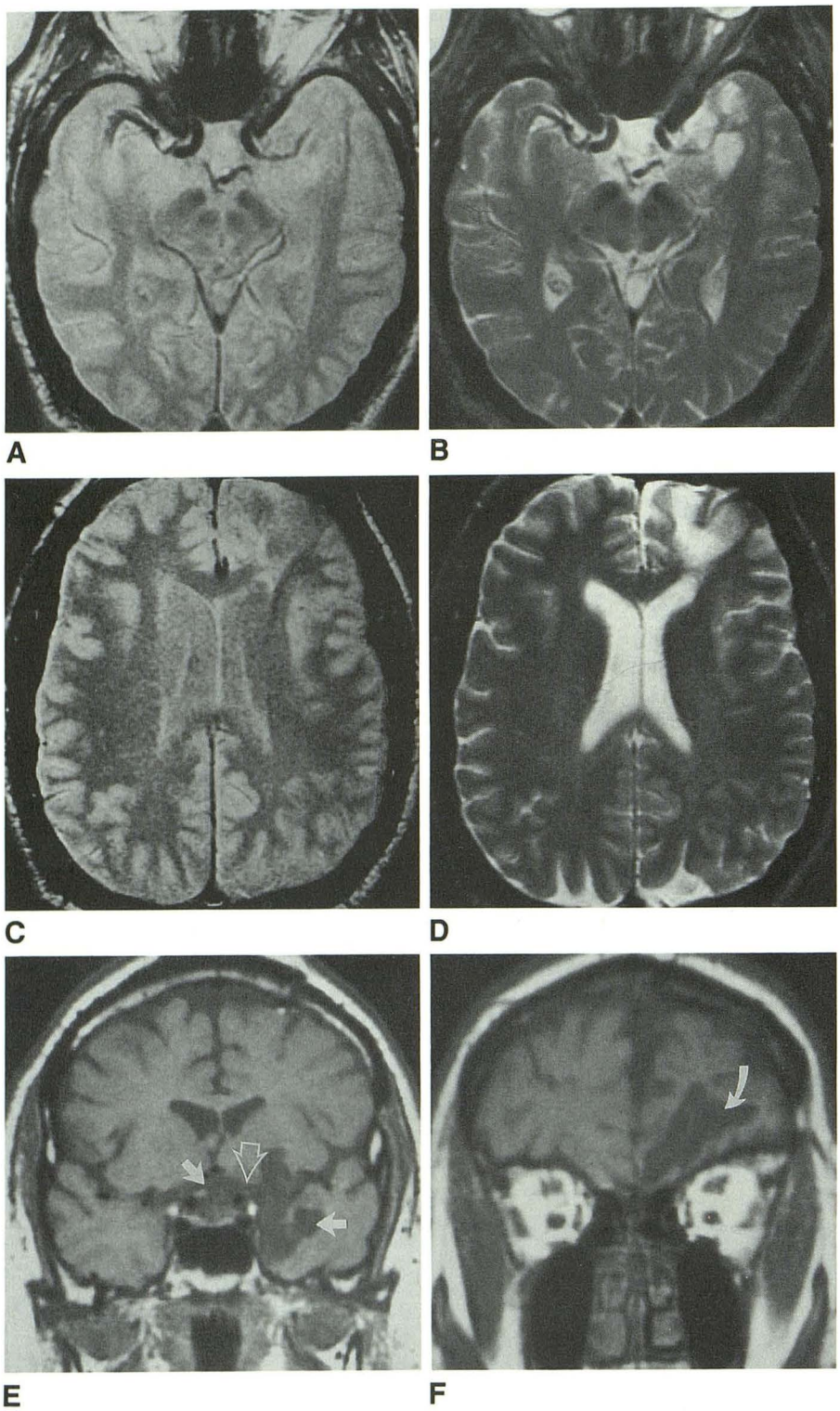


**Fig. 2.—Patient 2: Epidermoid tumor and postoperative encephalomalacia.**

***A–D*, Axial T2-weighted MR images (2800/30/80) show region of epidermoid tumor and encephalomalacia that is nearly isointense with CSF.**

***E* and *F*, Coronal T1-weighted MR images (600/20) show that the region of suspected tumor (*solid arrows* in *E*) cannot be easily separated from cisternal CSF (*open arrow* in *E*) or from frontal lobe encephalomalacia (*curved arrow* in *F*).**

**(Fig. 2 is continued on the opposite page.)**

2K–2M). Despite these limitations, diagnostic images were successfully obtained in all cases.

Physiological brain pulsations (up to 5 mm/sec) as a function of the cardiac cycle [11] have been observed in humans. These pulsations are several orders of magnitude greater than diffusion of water in the brain. Sensitivity to the pulsatile motion of the brain is unavoidable owing to the relatively long diffusion-gradient duration resulting in an echo delay time of 100 msec. These factors are required on our system in order to achieve high b values for our imaging sequences. These macroscopic motions are significant enough that measurements of diffusion coefficients of brain parenchyma may not be totally accurate [6]. An attempt was made to reduce physiological motion by the application of cardiac gating. The

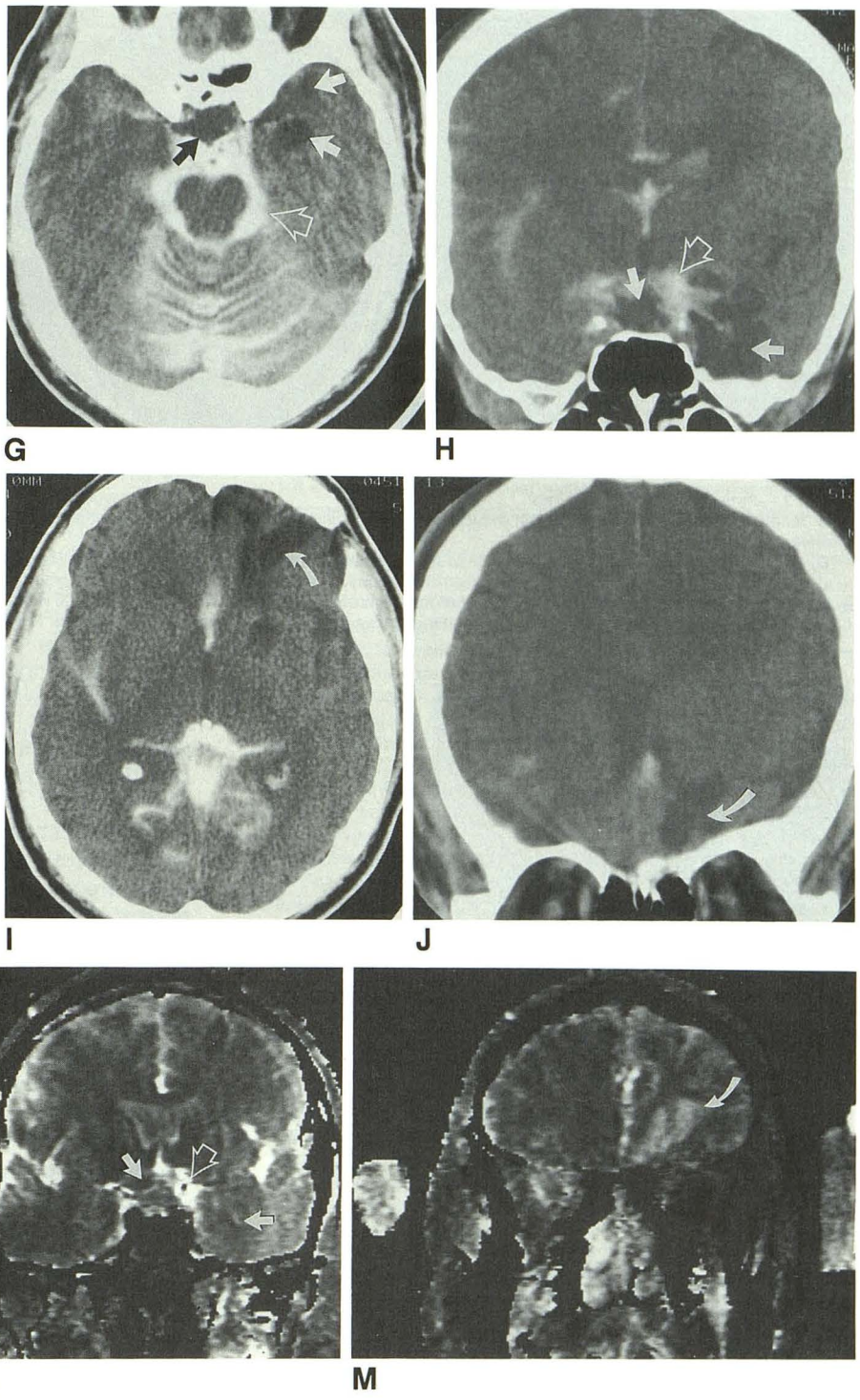


**Fig. 2—(continued).**

*G* and *H*, Axial (*G*) and coronal (*H*) CT cisternogram images show presence of a low-density mass (*solid arrows*) in suprasellar cistern extending into left middle cranial fossa. Note the normally enhancing basal cisterns (*open arrows*).

*I* and *J*, More anteriorly, axial (*I*) and coronal (*J*) CT cisternogram images depict an additional region of low density (*curved arrows*) within frontal lobe consistent with either postoperative encephalomalacia or epidermoid tumor.

*K–M*, Axial (*K*) and coronal (*L* and *M*) apparent diffusion coefficient (ADC) (gated/100) images show epidermoid tumor (*solid straight arrows*) with signal intensity that is isointense with brain parenchyma, indicating solid nature of mass. The high signal intensity of cisternal CSF (*open arrow* in *L*) correlates quite well with the normally enhancing CSF seen previously on CT cisternogram. The region of left frontal encephalomalacia (*curved arrow* in *M*) has intermediate intensity and is uniquely different from cisternal CSF, epidermoid tumor, and brain parenchyma. Note the shading artifact throughout the brain parenchyma, best appreciated on the coronal images, caused by patient motion. Marked heterogeneity and signal loss within lateral ventricles is noted on coronal ADC images, and presumably is due to complex CSF motion. Orbital motion degrades external phantom detail as a result of phase artifact.

contribution of tissue perfusion to the ADC may not be observed, since the capillary bed only represents a small fraction (<5%) [1] of the total brain volume and is overshadowed by macroscopic brain motion, which has similar velocity as capillary flow. In addition, macroscopic fluid motion—such as bulk, nonuniform CSF flow—is also a contributing factor to image degradation [7].

Since macroscopic motion significantly contributes to ADC image artifact, alternative methods for reducing the overall scan time have been proposed. These include CE-FAST [6], steady-state free precession [4], and echo planar imaging [12, 13]. For spin-echo imaging, adequate motion suppression has been obtained on a small-bore system in anesthetized animals [10]. In the present study, oral sedation (chloralhydrate) was used for patient 4 (Fig. 4) with favorable results. The additional use of signal averaging up to 8–16 times can also decrease apparent motion artifact [6]. However, signal averaging will increase total acquisition to an unacceptably

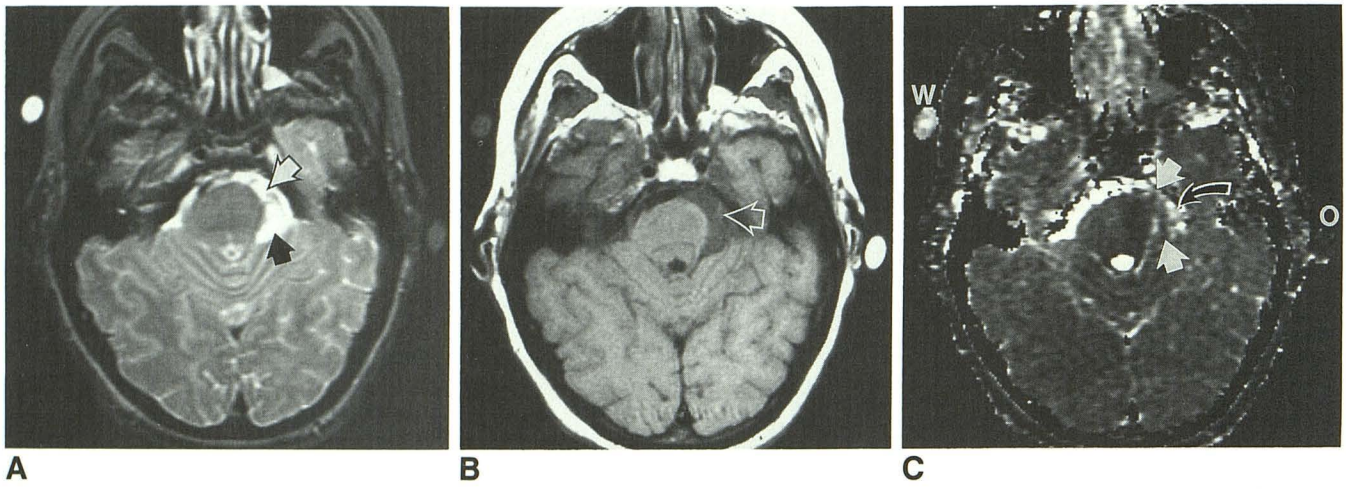


Fig. 3.—Patient 3: Epidermoid tumor.

*A*, Axial T2-weighted image (2800/80) depicts asymmetric widening of left cerebellopontine angle cistern by a lesion (*arrows*) with predominantly CSF intensity.

*B*, Axial T1-weighted image (600/20) confirms these findings. A portion of the left fifth cranial nerve can be identified (*open arrow*) within the lesion.

*C*, Apparent diffusion coefficient (ADC) (gated/100) study shows that this lesion (*straight arrows*) has similar signal intensity to the adjacent pons but quite distinct from either cisternal CSF or the stationary water phantom (W). The oil phantom (O) is also shown. The interface between tumor and cisternal CSF is well seen. Note that there appears to be minimal hyperintense CSF (*curved arrow*) lateral to mass.

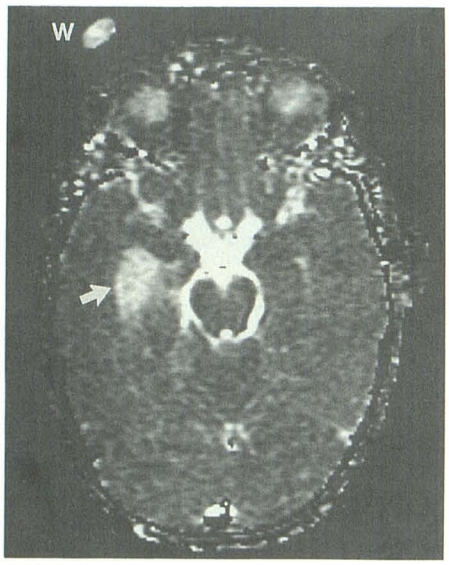


Fig. 4.—Suspected arachnoid cyst of right middle cranial fossa. Axial apparent diffusion coefficient (ADC) (gated/100) image confirmed that this lesion (*arrow*) has signal intensity similar to the water phantom (W). The lack of motion artifact was due to cardiac gating and patient immobilization. Slight heterogeneity was noted in the water phantom presumably due to truncation artifact.

long time for clinical application. To our knowledge, sequence optimization of spin-echo diffusion-weighted parameters, such as varying TR and gradient b values, in order to reduce motion artifact and improve signal-to-noise ratio has not been performed. This is an area that is currently under investigation in our laboratory.

Despite these limitations, we have noted that the ADC images have yielded consistently good results in delineating cisternal CSF. This is due to (1) the fast diffusion of CSF associated with water ($2.5 \times 10^{-5}$ $cm^2$/sec) [14]; (2) slowed diffusion associated with biological soft tissue, which is approximately 50% that of pure water [5]; and (3) macroscopic CSF flow, such as cisternal CSF, which further elevates its ADC over stationary water by up to 400% [2, 14]. From a quantitative standpoint, the differences in the ADC between brain parenchyma and CSF may be significantly different by several orders of magnitude. This potential for high dynamic range can be qualitatively seen on the ADC images as very high image contrast. In addition, any lesion that inhibits bulk CSF flow will be easily detected.

Variable success in obtaining homogeneously high signal intensity on the ADC images within the lateral ventricle was noted, presumably as a result of a greater degree of pulsatile motion leading to phase ghosting [6], especially if the flow is perpendicular to the imaging plane [7]. An example of this complex CSF flow artifact was noted in patient 2 (Fig. 2L). Phase artifact was also generated by orbital motion (Figs. 1D and 2K). This ghosting may be reduced with the application of gradient-moment nulling. Unfortunately, this technique was not available for our current diffusion-weighted sequences.

Determining tissue specificity on the basis of spin-echo images as well as calculated T1, T2, and proton-density values has been unreliable [15, 16]. In some cases complicated cysts may mimic solid neoplasms if there is alteration in protein content [17]. Additional factors such as the presence of paramagnetic substances may alter the signal intensity of cystic lesions [18]. Arachnoid cysts are typically isointense with CSF on all pulsing sequences [19–21] and are usually not a diagnostic challenge. Epidermoid tumors, on the other hand, may have variable signal intensity. According to some investigators [22–25], they are typically isointense or slightly hyperintense relative to CSF on both T1- and T2-weighted MR images. More definite diagnosis is valuable in

planning the optimal surgical approach [23]. In our experience, there are cases in which the MR signal intensity of epidermoid tumors may closely approach that of CSF, thus leading to diagnostic uncertainty and poor definition of the surgical anatomy. These difficulties were encountered in patients 2 and 3. CT cisternography may still be indicated in problematic cases.

ADC imaging yielded additional specificity in distinguishing between the cystic and solid nature of these tumors. External oil and water phantoms provided a more objective reference intensity value for identifying slowed diffusion within the epidermoid tumors. Improved delineation of the interface between the lesion and adjacent CSF was possible owing to the replacement of normally pulsatile cisternal CSF. In one sense, ADC imaging represents a physiological MR "cisternogram." In the second patient, ADC imaging, as compared with routine spin-echo MR and CT cisternography, was the only method that could distinguish between epidermoid tumor and postoperative encephalomalacia. While no definitive conclusions can be drawn from this single example, with improvements such as higher b values and/or faster imaging schemes, more valid conclusions on analyzing brain parenchyma may be obtainable while reliable quantitative diffusion numbers may provide additional tissue specificity. Furthermore, analysis of brain-water content may also be feasible. For example, initial studies have shown that early brain ischemia can be detected by changes in diffusion-restricted water and may function as an indicator of early cytotoxic edema [10].

## Conclusions

Our preliminary results show that diffusion-weighted MR imaging is helpful in characterizing and distinguishing between arachnoid cysts and epidermoid tumors that may be difficult to distinguish from CSF on spin-echo MR images. Improved differentiation of postsurgical changes was also possible. Several factors contribute to the increase in intensity of cisternal CSF on the ADC images, most importantly bulk flow. This effect will enhance image contrast between normally pulsatile CSF and nonpulsatile extraaxial tumors. Proper patient immobilization is important. Despite limitations imposed by macroscopic motion, we have adopted this technique as a routine tool in further characterizing challenging extraaxial lesions.

ACKNOWLEDGMENTS

We thank James R. MacFall and Ann Shimakawa for their support and helpful comments.

REFERENCES

1. Le Bihan D, Breton E, Lallemand D, Aubin M-L, Vignaud J, Laval-Jeantet M. Separation of diffusion and perfusion in intravoxel incoherent motion MR imaging. *Radiology* **1988**;168:497–505
2. Chien D, Buxton R, Rosen B, Johnson K. MR imaging of restricted diffusion in biological systems. *Proceedings of annual meeting Soc Magn Reson Med*, New York City, **1987**:887
3. Le Bihan D, Breton E, Lallemand D, Grenier P, Cabanis E, Laval-Jeantet M. MR imaging of intravoxel incoherent motions: application to diffusion and perfusion in neurologic disorders. *Radiology* **1986**;161:401–407
4. Le Bihan D. Intravoxel incoherent motion imaging using steady-state free precession. *Magn Reson Med* **1988**;7:346–351
5. Le Bihan D, Breton E, Lallemand D, Brugieres P, Gueron M. Tissue characterization by molecular diffusion using intravoxel incoherent motion (IVIM) MR imaging. *Proceedings of annual meeting Soc Magn Reson Med*, San Francisco, **1988**:306
6. Merboldt K-D, Bruhn H, Frahm J, Gyngell M, Hanicke W, Deimling M. MRI of "diffusion" in the human brain: new results using a modified CE-FAST sequence. *Magn Reson Med* **1989**;9:423–429
7. Thomsen C, Henriksen O, Ring P. In vivo measurement of water self diffusion in the human brain by magnetic resonance imaging. *Acta Radiol* **1987**;28:353–361
8. Thomsen C, Gjerris F, Sørensen S, Ring P, Henriksen O. Increased water self diffusion in the brain white matter in patients with abnormal CSF hydrodynamics. *Proceedings of annual meeting Soc Magn Reson Med*, San Francisco, **1988**:118
9. Carr H, Purcell E. Effects of diffusion on free precession in nuclear magnetic resonance experiments. *Physiol Rev* **1954**;94:630–635
10. Cohen Y, Mintorovitch J, Chileuitt L, et al. Early detection of ischemic injury: comparison of diffusion and T2-weighted MRI and spectroscopy during regional cerebral ischemia in cats. *Proceedings of annual meeting Soc Magn Reson Med*, Amsterdam, **1989**:42
11. Feinberg D, Mark A. Human brain motion and cerebrospinal fluid circulation demonstrated with MR velocity imaging. *Radiology* **1987**;163:793–799
12. Le Bihan D, Turner R, MacFall J. Artifacts in intravoxel incoherent motion (IVIM) MR imaging. *Proceedings of annual meeting Soc Magn Reson Imaging*, Los Angeles, **1989**:172
13. Turner R, Le Bihan D, Delannoy J, Pekar J. Echo-planar diffusion and perfusion imaging at 2.0 Tesla. *Proceedings of annual meeting Soc Magn Reson Med*, Amsterdam, **1989**:139
14. Le Bihan D, Breton E, Barth M, Aubin M, Lallemand D, Vignaud J. CSF flow and diffusion mapping using intra-voxel incoherent motion (IVIM) imaging. *Proceedings of annual meeting Soc Magn Reson Med*, New York City, **1987**:313
15. Komiyama M, Yagura H, Yasui T, Hakuba A, Nishimura S, Inoue Y. MR imaging: possibility of tissue characterization of brain tumors using T1 and T2 values. *AJNR* **1987**;8:65–70
16. Just M, Thelen M. Tissue characterization with T1, T2, and proton density values: results in 160 patients with brain tumors. *Radiology* **1988**;169:779–785
17. Haimes A, Zimmerman R, Morgello S, et al. MR imaging of brain abscesses. *AJNR* **1989**;10:279–291
18. Hackney D, Grossman R, Joseph P, Goldberg H, Bilaniuk L, Spagnoli M. Low sensitivity of clinical MR imaging to small changes in the concentration of nonparamagnetic protein. *AJNR* **1987**;8:1003–1008
19. Harsh G, Edwards M, Wilson C. Intracranial arachnoid cysts in children. *J Neurosurg* **1986**;64:835–842
20. Wiener S, Pearlstein A, Eiber A. MR imaging of intracranial arachnoid cysts. *J Comput Assist Tomogr* **1987**;11:236–241
21. Garcia-Bach M, Ismat F, Vila F. Intracranial arachnoid cysts in adults. *Acta Neurochir Suppl* (Wein) **1988**;42:205–209
22. Vion-Dury J, Vincentelli F, Jiddane M, et al. MR imaging of epidermoid cysts. *Neuroradiology* **1987**;29:333–338
23. Olson J, Beck D, Crawford S, Menezes A. Comparative evaiuation of intracranial epidermoid tumors with computed tomography and magnetic resonance imaging. *Neurosurgery* **1987**;21:357–360
24. Steffey D, De Filipp G, Spera T, Gabrielsen T. MR imaging of primary epidermoid tumors. *J Comput Assist Tomogr* **1988**;12:438–440
25. Tamperi D, Melanson D, Ethier R. MR imaging of epidermoid cysts. *AJNR* **1989**;10:351–356

The reader's attention is directed to the commentary on this article, which appears on the following pages.